Pergamon

Int. J. Impact Engng, Vol. 17, pp. 263–274, 1995
Elsevier Science Ltd
Printed in Great Britain
0734-743X/95 $9.50+0.00

PERFORMANCE OF MODEL SCALE LONG ROD PROJECTILES AGAINST COMPLEX TARGETS OVER THE VELOCITY RANGE 1700-2200 M/S

I. G. Cullis and N. J. Lynch

Defence Research Agency, Fort Halstead
Sevenoaks, Kent TN14 7BP, England

Summary-This paper presents an investigation into the performance of homogeneous and non-homogeneous targets using a quarter scale long-rod penetrator (LRP) over the velocity range 1700-2200m/s. Use has been made of an Eulerian hydrocode to provide performance predictions and assist in the analysis of material interactions. Results of the trials are presented and some comparisons made with the hydrocode analysis. Additionally, the effect of improvements in material models and advection routines used in the hydrocode are discussed. The agreement between experiment and simulation is shown to be very good, providing an explaination for the experimental observtaions.It is also concluded that the use of semi-infinite RHA backing plates can be misleading due to the nonlinearity of RHA penetration below 600m/s and above 1800 m/s. In the case of targets containing ceramic elements penetration depth is observed to be linear with velocity up to 2200m/s. Although simple ceramic material models are capable of reproducing the depth of penetration in the backing armour, they are unable to reproduce the conditions within the ceramic during and after penetration.

BACKGROUND

The numerical and experimental study of penetration mechanics is vitally important to both the warhead designer and the armourer. Demands for improved performance require that physical processes, considered second order, have to play a dominant role in the design.

The aim of the long term research programmes into warhead design, armour development and materials within the DRA is to replace these full scale trials with a more extensive series of scaled experiments linked to hydrocode simulations. The simulations can then be used to predict the full scale performance validated against a much more limited series of full scale trials. The use of scaled trials also permits the full range of diagnostic techniques to be applied to the experiments, hence supplying important data to validate the hydrocodes.

With the advent of the electro-magnetic gun, strike velocities of LRPs up to 3000m/s appear to be possible, but the performance against the types of armour which would be fielded against them, is still largely unknown. Analytical theory such as the modified Bernoulli formulae developed by Tate [1] and experimental work by Hohler and Stilp [2] against semi-infinite RHA (Rolled Homogeneous Armour) indicated that the linear relationship between velocity and penetration depth would start to level off at 1700-1800m/s and plateau at 2200m/s. It was by no means clear that the same case was true for armours containing non-metallic materials such as ceramic and Glass Reinforced Plastic (GRP). The experimental work described here covers the velocities from 1700 to 2200m/s representing the transition from powder

guns to the hypervelocity regime.

The primary aim of the associated hydrocode simulations, therefore, was to understand the dominant physical processes and hence explain the observed performance trends with increasing penetrator velocity. In addition the ability of a number of material models including a microscopically based constitutive model to represent the experimental results were investigated.

EXPERIMENTAL WORK

A W-Ni-Fe projectile with an aspect ratio (l:d) of 12:1, and a diameter of 6mm, was fired at velocities between 1700m/s and 2200m/s using the 40mm calibre, 9 metre long barrel gun at Fort Halstead. The projectile weighed 35 grams and was launched using a low cost nylon sabot, base push, shot design. Two rounds were fired at each velocity to improve the reliability of the results.

A 150mm cube of RHA (rolled homogeneous armour) at 0° obliquity, and a 90mm thick plate at 65° obliquity were used to obtain a baseline performance for the projectile, and for calculating target effectiveness (Em) values.

A RHA/ceramic/GRP/RHA target was chosen to represent a typical non-homogeneous RHA armour. The arrangement of the target is shown in Figure 1.

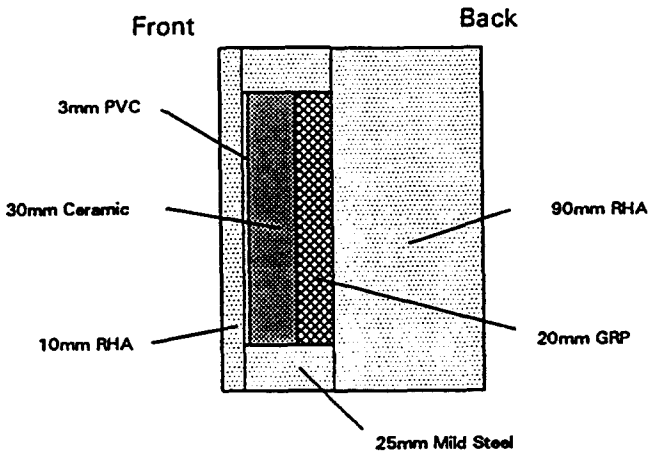

Figure 1
Confined ceramic target

The ceramic tiles were 20cm square and 3 cm thick Deranox 975, a 97.5% Al_2O_3. The assembly was potted in Permabond E27, a low viscosity epoxy cement, to reduce the influence of tensile reflections from air gaps. The ceramic/GRP assembly was contained in 25mm of welded steel confinement and clamped to the front and rear RHA elements with eight M8 tie bolts.

To provide experimental data for hydrocode modelling, two rounds were fired at 1950m/s against a multi-plate target consisting of 5 layers of 4mm RHA inclined at 65° and with an air gap between the layers of 4mm. The target was mounted onto a thick RHA backing to obtain residual penetration data.

RESULTS

Baseline RHA- The 0° RHA results showed the expected fall-off in penetration for unitary rods above 1700m/s. The experimental results are shown in Figure 2 compared with results at lower velocities obtained from earlier work at Fort Halstead.

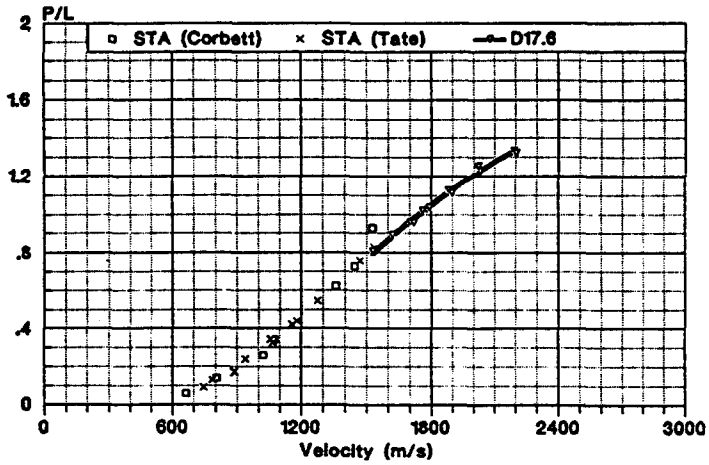

Figure 2. Experimental Penetration efficiency against zero degree semi-infinite RHA for a L:D=12 Penetrator

The 65° RHA results are shown in Figure 3, with details tabulated in Table 1a. There is a surprising reduction in penetration above 2100m/s which cannot be accounted for by projectile yaw. All the RHA was obtained from the same batch of material and even for the deepest penetration there was no evidence of bulging in the RHA material.

There is little reported work on oblique semi-infinite impact, since apart from the initial entry effect, the projectile should act as at normal incidence. With high obliquity angles the projectile is close to the free front surface of the target and there is a tendency for the projectile to deviate towards it. The hydrocode analysis allowed a more detailed study of these penetration features, and was able to explain them.

There are a number of methods for measuring oblique penetration depth. Either, a) in line depth from the point of impact, b) in line depth along the centre-line of the resulting crater, or c) a cosine of the penetrated depth normal to the plate surface. Method c is now accepted practice and that measurement is used in this analysis.

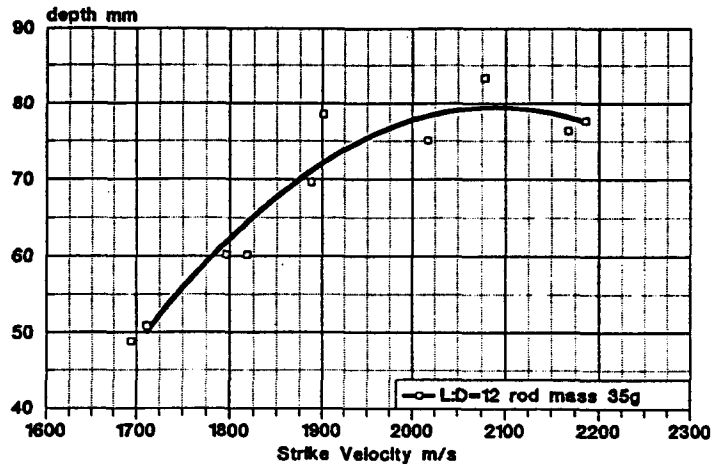

Figure 3. Experimental In line penetration into semi-infinite 65° RHA

CERAMIC LAMINATE

The penetration depths for the ceramic target are shown in the lower curve in Figure 4 (the solid line represents a best fit polynomial). There was more scatter in the penetration depths than the semi-infinite RHA, particularly at the higher velocities. From previous tests it has been found that the ceramic

performance is very dependant on the quality of mechanical coupling between the target elements. Work at DRA Chertsey [3] using various potting cements, under vacuum filling, showed that DoP was relatively insensitive to the cement used, though the degree of comminution in the ceramic was quite different. Whilst the welded containment around the ceramic remained intact up to a velocity of about 2000m/s, at velocities higher than this the welded containment fractured but this does not appear to have reduced the effectiveness of the target.

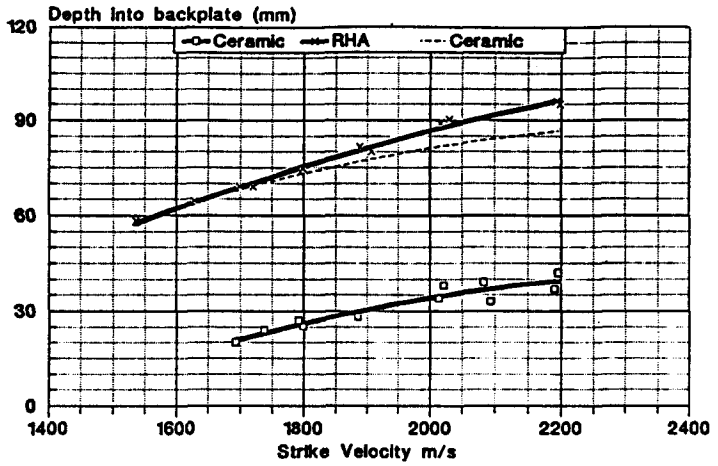

Figure 4. Experimental Penetration depths for 0° semi-infinite RHA and ceramic laminate for an L:D=12 Penetrator

The upper curves in Figure 4 compare the 0° RHA data with the ceramic results, which have been transposed by a constant 47mm (dotted line). The comparison suggests that the rate of increase of penetration with velocity is not as high for the ceramic target as it is into RHA. In order to satisfactorily compare the Depth of Penetration (DoP) results from the different target designs the residual velocity should be within the linear range of the RHA penetration curve, ie 1100 to 1800m/s. Estimating the depth of penetration using a Tate linear fit prediction, the residual velocities into the backplate were calculated to lie between 1400 and 1800m/s. A differential mass effectiveness factor, Em, for the target was calculated from the formulae:

$$E_m = \frac{\rho_0 (P_{ref} - P_{res})}{\rho_t \cdot P_t} \tag{1}$$

Where:

ρ_0	is the RHA density
ρ_t	is the density of the non-RHA element
P_{ref}	is the reference penetration depth into RHA
P_{res}	is the residual penetration into the RHA backing
P_t	is the thickness of the non-RHA element

To allow for the cover plate and GRP the equation now becomes:

$$E_m = \frac{\rho_0 (P_{ref} - (P_c + P_{res}))}{(\rho_1 \cdot P_1) + (\rho_2 \cdot P_2)} \tag{2}$$

Where P_c is the cover plate thickness and suffixes 1 and 2 represent the ceramic and GRP elements of the target. The variation of Em with strike velocity is shown in Figure 5. An indication is that the target is becoming increasingly efficient, with respect to RHA, as velocity increases, agreeing with the reduced rate

of increase in penetration with velocity observed in Figure 4.

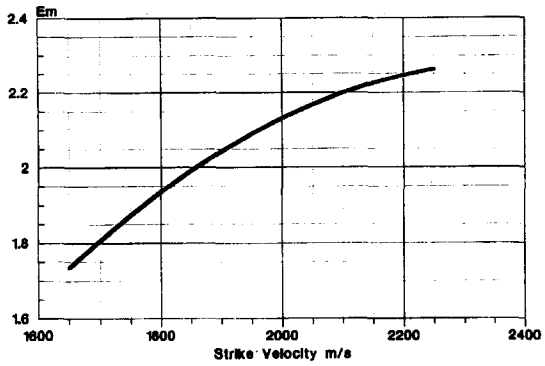

Figure 5. Ceramic laminate. Variation of Em with velocity for an L:D=12 Penetrator

HYDROCODE ANALYSIS

The Eulerian code GRIM, developed by the Warheads division of the DRA, was employed in the study. GRIM2D was employed to study the zero obliquity RHA and ceramic targets and GRIM3D for an assessment of the 65° obliquity RHA and multiplate targets.

Successful hydrocode simulations must be capable of resolving the controlling aspects of the flow field and be able to predict the onset and development of material dependent process, eg fracture and plastic instabilities. To achieve this demands a realistic material model. The ability of a hydrocode simulation to accurately reproduce an experimental observation is directly proportional to the realism of the material description used.

SEMI INFINITE PENETRATION STUDIES

The numerical meshes employed in both the 2D and 3D simulations had the same linear dimension of 1 mm. A higher order advection scheme was employed, since previous work with GRIM and the HULL code had shown that in general the use of a first order advection scheme leads to an under prediction of penetration performance of about 10% at lower velocities increasing to about 15% to 20% at higher velocities. These findings are also sensitive to the penetrator target configuration. As will be shown below the use of a higher order advection scheme can resolve quite sensitive penetrator-target interaction effects even on coarse numerical meshes.

MATERIAL MODELS

Two fundamentally different material constitutive models were used in the study, an elastic-perfectly plastic model, referred to as the HULL model, and the modified Zerilli-Armstrong due to Goldthorpe, referred to as the AZ model [4].

The HULL model is phenomenological. It assumes the work hardening and thermal softening associated with plastic deformation can be treated independently. Since in many detonics and terminal ballistics scenarios materials rapidly work harden, strain rate effects are assumed to be contained in the work hardened flow strength. The parameters used for RHA and the tungsten alloy (92.5% W-Ni-Fe-Co) are derived from Taylor tests and penetration simulations at velocities around 1700 m/s [5]. For a narrow design envelope it remains a very useful model, particularly where materials may not be well defined. The

material constants for the HULL model are listed in Table 2.

The AZ model, however, is based on fundamental concepts associated with dislocation mechanics and their influence on microstructural behaviour. It attempts to relate the material structure to its observed deformation behaviour. The work hardening, strain rate dependency and thermal softening behaviour follow as a natural consequence of the theory.

Early work at DRA [6], showed the AZ model to have distinct advantages over existing constitutive models. In particular the model demonstrated the importance of pre-shocking in altering the structure of the material and hence its deformation behaviour. At a fundamental level since the model is fitted to a series of independent material tests its use in hydrocode simulations adds credibility to the predictions of the calculations. The interesting observation, however, was that for the soft iron being used for EFP's the same rate dependency applied to both the unshocked and shocked material. Recent work, by Goldthorpe, Butler and Church [7], has extended this finding to a number of RHA's and hard steels, suggesting that a generic material model can be developed for unshocked iron and steels. The resulting modified algorithm for RHA with a hardness of H_v 300 is :

$$\sigma = C_2 e^{(C_3 T + C_4 T \log \dot{\epsilon})} + (C_1 + C_5 \epsilon^n) * (1.13 - 0.000445 T) \qquad (3)$$

where σ = Flow stress; ϵ = Effective plastic strain; $\dot{\epsilon}$ = Effective plastic strain rate; T = Temperature

and $C_1 = 650$ MPa; $C_2 = 625$MPa; $C_3 = -0.00344$; $C_4 = 0.000263$; $C_5 = 590$ Mpa; $n = 0.41$

The discovery that a generic algorithm can be applied to a material in different metallurgical conditions represents a breakthrough in material science and considerable potential for hydrocode modelling.

2D STUDIES

The results, using the HULL and AZ material models are shown in figures 6 and 7 respectively. Also in figure 7 are the penetration of the same tungsten alloy as a KE penetrator with a diameter of 10.6mm and a length of 45mm (l:d=4.2) over a range of velocities from 1200 m/s to 2200 m/s. For both material models the penetration depth was found to be surprisingly insensitive, less than 4%, to a change in cell size of a factor of 2, independent of velocity. Comparison with experiment is in general excellent, within 2%.

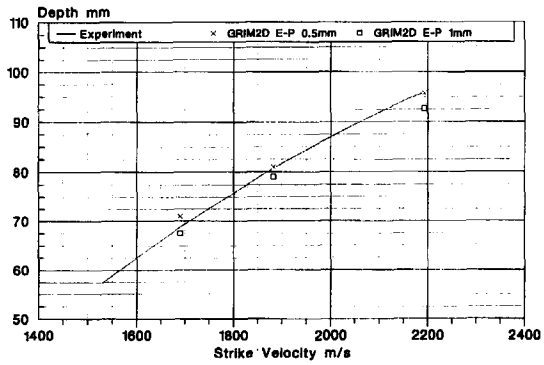

Figure 6: Experimental and computed (HULL model) penetration depths in RHA L:D=12 penetrator

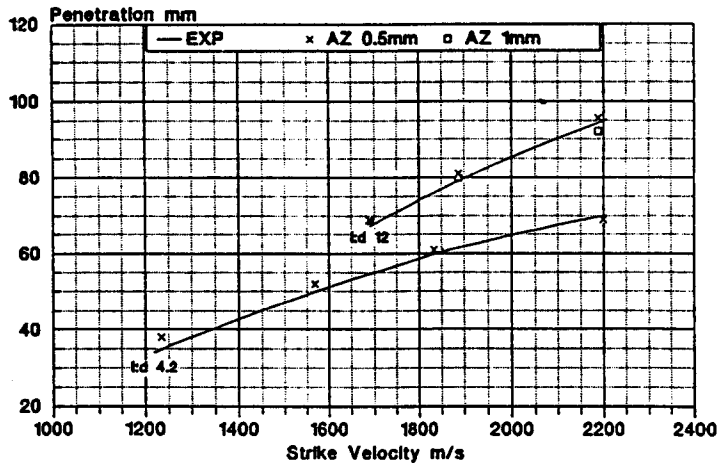

Figure 7. Experimental and computed, using Armstrong-Zerilli models, penetration depths in semi-infinite RHA L:D=12 Penetrator

3D STUDIES

The semi-infinite penetration performance of the same penetrator at an obliquity of 65° was investigated using a GRIM3D mesh containing 200x260x50 cells requiring typical cpu times of 8 to 16 hours to reach 100 μs depending on the complexity of the problem. The results are presented in Table 1a.

Using the HULL model the predicted crater profiles are directly compared with the experimentally observed profiles in Figure 8. In general the agreement is very good although now the best agreement is at 1900 m/s and not at 1600 m/s, as in the 2D simulations. The characteristic bending of the crater axis towards the free surface of the RHA block is reproduced very well at the lower velocities but less well at the highest velocity. These results demonstrate the inadequacies of the HULL type material models at the higher velocities. Whilst the prediction of the symmetric crater profiles observed in normal impact is excellent the prediction of the asymmetric crater profiles associated with oblique impact is not as good. The sensitivity of the curvature of the profile to material properties is quite marked and is more sensitive to the properties of the penetrator than the target.

As the impact velocity increases the inertial resistance of the target is unable to prevent the flow of penetrator material between the penetrator and the target. The degree of asymmetry in the flow field is therefore reduced, which in turn reduces the rotation of the penetrator away from its initial trajectory.

The normal penetration depth as a function of impact velocity exhibits a typical S-shaped profile which represents a balance between the inertial resistance of the target, penetrator momentum and strength effects. As the impact velocity increases the contribution to the final penetration depth due to the residual penetrator mass and target afterflow increases. In the case of oblique incidence, however, these late stage penetration processes will be directed away from the initial trajectory as shown by the simulations. It is these mechanisms that account for the experimentally observed fall off in final penetration depth with increasing velocity.

MULTI-PLATE TARGET STUDIES

Having satisfactorily demonstrated the ability of GRIM to reproduce the semi-infinite penetration results simulations were performed on a single plate and a multi plate target array. The objective of the simulations was to establish the ability of GRIM to describe the interaction of a KE penetrator with

discrete target elements. It is well known [8] that it is the interaction with single target elements that often leads to the dynamic bending and breakup of the penetrator. Whilst it was recognised that the coarse mesh resolution and the lack of a detailed failure model would be unable to predict the breakup and failure of the penetrator, it was hoped that the simulations would identify the important mechanisms responsible and their sensitivity to mesh resolution.

SINGLE PLATE

The 3D simulation studied the effects of the asymmetric target orientation on the trajectory of the projectile. The results are shown in Figure 9. The projectile length is reduced by 14mm. The effect of the breakup of the plate at right angles to its rear surface and the interaction of the edge of the hole with the front of the projectile leads to the front of the projectile bending towards the rear surface of the plate. This should be contrasted with the semi-infinite case where the rod bends in the other direction towards the free surface of the block. Thus the importance of the release waves in, and inertial mass of, the target in controlling the bending of the penetrator is explained.

The ability of GRIM3D to reproduce the bending of the rod on a quite coarse mesh has been demonstrated. A simulation with the first order advection scheme failed to resolve the interaction of the rod with the plate and the details of the velocity distribution within it.

MULTI-PLATE

The multiplate array was also simulated with the 65^0 angle of obliquity. The results are shown in Figure 10 where the co-operative effect of the plates in turning the projectile is readily apparent. The loss in length of the penetrator, however, at 48mm, is considerably less than the 70mm that would be expected from a simple additive law for single plates. The deflection of the rod is clearly a function of plate thickness, spacing and rod velocity. By analysing the simulations in this way the need for experiments to make relevant measurements of the condition and orientation of the emerging projectile, rather than the semi-infinite penetration are highlighted. Such measurements are essential for cost effective armour design studies using a 3D Eulerian code .

It is interesting to observe that the rotation of the projectile as it emerges from the array, implies its Em value, based on the residual penetration in the backing armour, will be a function both of the spacing and orientation of the backing armour.

Since the experiment measured the performance in a 90mm block of RHA 4mm behind the multi-plate array, the simulation was repeated to include this 90mm thick block. The predicted final penetration in the RHA block of 12mm is somewhat greater than the 8mm measured experimentally and detailed in Table 1c. The final target-penetrator orientation at 90 μs is also shown in Figure 11.

CERAMIC LAMINATE TARGET

The penetration performance of the KE projectile at normal incidence against the ceramic laminate target described above and illustrated in Figure 1 was simulated using GRIM2D. It is well known that ceramics exhibit a very complex response to dynamic loading conditions. At the time of this study, however, an advanced model for ceramics [9] was unavailable. A simple Mie-Gruneisen equation of state with a HULL type constitutive model was therefore, used to represent the ceramic. The material properties used are presented in Table 2. The simulations were performed at three impact velocities, 1750m/s, 2021m/s and 2195m/s. The last two were compared directly with velocities from experimental data.

The results are compared with the experimental results in Table 1b. Whilst the final penetration depth into the RHA backing armour is in remarkable agreement with the experiments there is a distinct trend for the simulations to over predict the DoP with increasing velocity. Whilst the difference is very small the

simulation results lie on the extreme of the experimental spread at a given velocity. In addition the difference would become significant for predicting full scale performance.

Comparison of other details of the target response however are in less good agreement with experiment. Whilst the hole sizes in the cover plate, GRP and backing armour are in very good agreement with observation the condition of the ceramic is poorly represented. In particular the experimentally observed powdered region surrounding the projectile trajectory extends out to a radius of 50 mm with ever increasing rubble size out to the side containment. The simulation, given the inadequate material model fails to reproduce this at all. The evidence of bulking in the pulverised ceramic, whilst effecting the bulge in the front plate appeared not to affect the final penetration depth in the backing armour. Clearly more research is required to develop an improved model that introduces the enhancement of the flow stress with confinement, the damage mechanisms that reduce it and the bulking process that can further interact with the projectile. Ultimately a successful algorithm must reproduce the observed sensitivity to projectile yaw.

Since many of these mechanisms dominate in oblique impact situations the planned 3D simulations were not performed. Nevertheless the 2D simulations demonstrate that a simple model can reproduce the DoP results in simple symmetric target geometries provided the ceramic model can reproduce the average resistance to penetration. Since this resistance is a function of velocity, however, the model would have to be fitted to a specific velocity range and target configuration.

CONCLUSIONS

The use of a semi-infinite RHA backing plate to measure residual penetration can be misleading due to the nonlinearity of RHA penetration below 600m/s and above 1800m/s. As the strike velocity increases, the target becomes increasingly overmatched, and hence the percentage of resistance to penetration contributed by the complex target becomes less. Adding elements to the target at higher velocities would make it difficult to compare results across the whole range of velocities.

Model scale results indicate that the penetration depth of a zero obliquity Ceramic/GRP laminate increases linearly with velocity up to 2200m/s.

The depth of penetration in the semi-infinite targets predicted by GRIM hydrocode simulations were shown to be in good agreement with experiment. The simulations were able to explain the observed increased fall off in penetration at higher velocities for oblique targets.

The material models were shown to be relatively insensitive to mesh size with the modified Armstrong Zerilli model appearing better able to predict penetration over a wide velocity range compared to a simple elastic perfectly plastic algorithm.

For the thin plate arrays and projectile velocities considered the perforation mechanisms were treated quite well. In general, however, their simulation by hydrocodes is non-trivial and requires considerable further research.

Simple material models for ceramics have been shown capable of reproducing the depth of penetration in the backing armour, but not the details of the conditions in the ceramic during and after penetration. Further extensive materials research is again required.

REFERENCES

1 A Tate. Further results in the theory of long rod penetration. J Mech Phys Solids, Vol 17, (1969) pp141-150.

2. Hohler and Stilp. Hypervelocity impact of rod projectiles with L/D from 1 to 32. Int.J Impact

Engng., Vol 5, (1987) pp323-331.

3. B J James. Initial results of full confinement trials on ceramic ballistic targets. DRA/FV&S/AM/WP93004/1.0 October 1993.

4. B. D. Goldthorpe. Constitutive Equations for Annealed and Explosively Shocked Iron for Application to High Strain Rates and Large Strains. DYMAT Conference; J. De Phys. IV, suppl to J De Phys. III, Vol 1 pp C3/829-835, 1991

5. I G Cullis, N J Lynch. Hydrocode and Experimental Analysis of Scale Size Jacketed KE Projectiles. 14th International Symposium on Ballistics, Quebec, Canada. pp 271-280. 1993

6. I G Cullis. Experiments and Modelling in Dynamic Materials Properties: Explosively Formed Projectile Research in a European Collaborative Forum 13th International Symposium on Ballistics, Stockholm, Sweden, Vol 1, GS-3, pp55-62

7. B D Goldthorpe, P Church, A. Butler. A wide range constitutive equation for medium nad high strength steels. International Conference on Mechanical and Physical Behaviour of Materials under Dynamic Loading. Oxford, September 1994. (to be published)

8. M Borrmann, H J Raatschen, M Holzner Numerical Investigations Concerning the Transferability of Small to Full Scale Experiments. 13th International Symposium on Ballistics, Stockholm, Sweden, Vol 3, TB-8, pp65-66

9. W A J Carson, I G Cullis, J Cagnoux, M Cauret et al. Penetration of Alumina ceramics by tungsten rod projectiles. 14th International Symposium on Ballistics, Quebec, Canada. pp545-554. 1993

Round No.	Velocity (m/s)	Yaw (degrees)	Penetration (mm)		Penetration. GRIM3D	
			at normal	in line (65°)	at normal	in line (65°)
X226	1695	0.7	20.6	48.9	20	32
X223	1712	1.5	21.5	50.9		
X224	1796	1.4	25.4	60.2		
X227	1819	-0.3	25.4	60.2		
X225	1888	1.1	29.4	69.6	34	76
X229	2000	n/r	33.2	78.6		
X230	2017	0.1	31.7	75.1		
X231	2078	0.2	35.2	83.3		
X233	2168	-2.8	32.3	76.4		
X234	2186	0.1	32.8	77.7	40	90

Table 1a. 65° Semi-infinite. Experiment and hydrocode analysis

Round No.	Velocity (m/s)	Yaw (degrees)	Penetration into backplate (mm)	Hydrocode (mm)
X249	1737	-0.9	24	24 @ 1750m/s
X250	1799	1.4	25	
X254	2021	1.1	38	40 @ 2021m/s
X255	2015	2.1	34	
X258	2190	1.4	37	45.6 @ 2190m/s
X259	2195	0.9	42	

Table 1b. Ceramic target experiments and hydrocode analysis

Round No.	Velocity (m/s)	Yaw (degrees)	Depth in rear RHA (mm)	Hydrocode (mm)
X240	1925	-3.5	8.2	12.0 @ 1950m/s
X241	1950	0.2	8.0	

Table 1c. Multiplate target. Experiment and hydrocode analysis

Material	Rho kg/m³	C Km/s	S	Γ	I x10⁴ J/kg	G GPa	Y(E) MPa	HULL type softening data		
								θ_1 I_1	θ_2 I_2	θ_3 I_3
Tungsten	17600	4.0	1.268	1.58	2.626	133.96	2000	1, 2.626	0.9, 10.38	0, 22.35
RHA	7860	4.61	1.73	1.67	7.556	95	1370	1, 7.556	0.9, 47.63	0, 87.7
Ceramic	3800	6.6	1.636	1.30	7.95	114.3	1750	1, 7.95	0.5, 100	0, 200
GRP	2200	3.276	1.05	0.32	7.95	11.79	300	1, 7.95	0.5, 100	0, 200

Table 2. Material constants for constitutive models used in the analysis

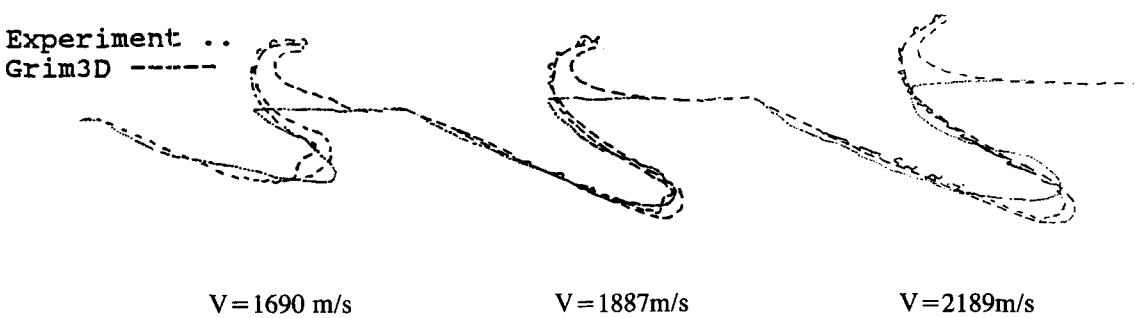

Figure 8 : Predicted and experimental crater profiles in RHA: Penetrator L:D=12

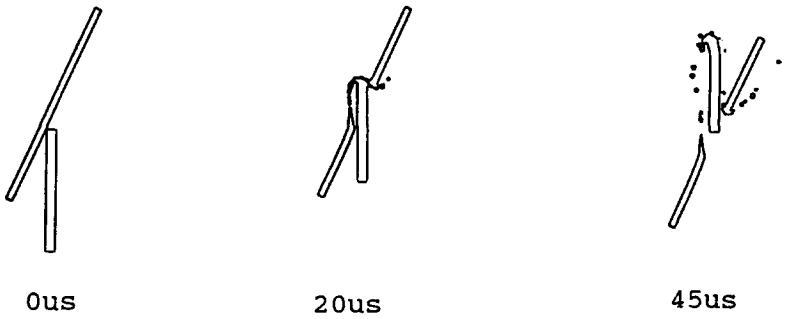

Figure 9 : GRIM3D simulation L:D=12 penetrator, V=1950 m/s: 5mm RHA plate target

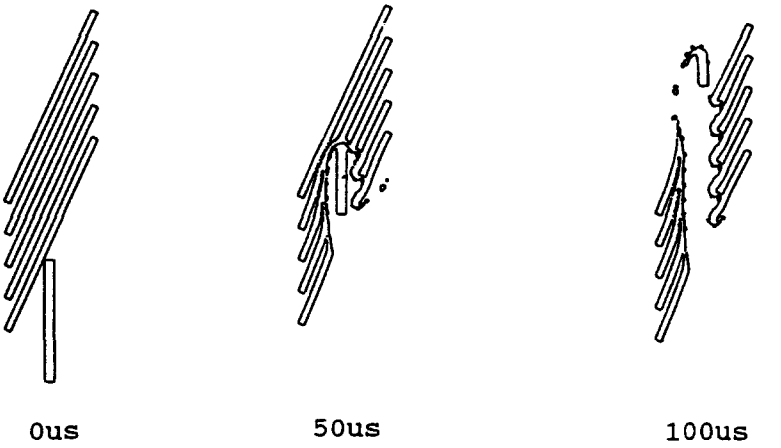

Figure 10 : GRIM3D simulation L:D=12, V=1950 m/s: 5 mm RHA multiplate target

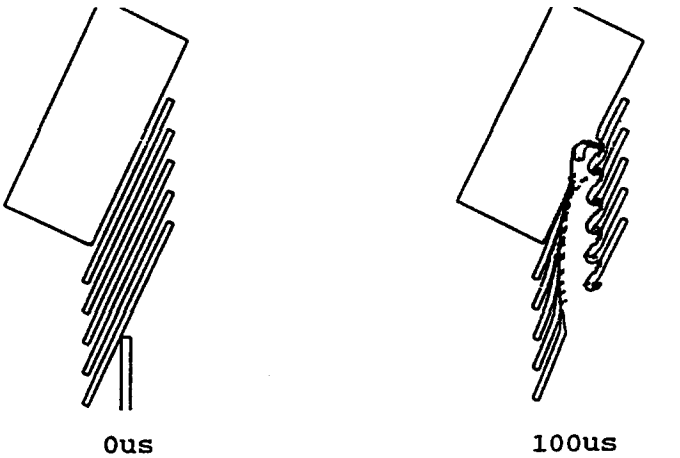

Figure 11 : GRIM3D simulation L:D=12, V=1950 m/s: RHA multiplate + backing RHA

Defence Research Agency
Farnborough, Hants GU14 6TD